Downloaded from orbit.dtu.dk on: May 05, 2023

DTU Library

The Effect of Nano-TiC Addition on Sintered Nd-Fe-B Permanent Magnets

Mural, Zorjana ; Kollo, Lauri ; Xia, Manlong; Bahl, Christian; Abrahamsen, Asger Bech; Neves Bez, Henrique; Link, Joosep ; Veinthal, Renno

Published in:
Journal of Magnetism and Magnetic Materials

Link to article, DOI:
10.1016/j.jmmm.2016.12.115

Publication date:
2017

Document Version
Peer reviewed version

Link back to DTU Orbit

Citation (APA):
Mural, Z., Kollo, L., Xia, M., Bahl, C., Abrahamsen, A. B., Neves Bez, H., Link, J., & Veinthal, R. (2017). The Effect of Nano-TiC Addition on Sintered Nd-Fe-B Permanent Magnets. *Journal of Magnetism and Magnetic Materials*, *429*, 23–28. https://doi.org/10.1016/j.jmmm.2016.12.115

General rights
Copyright and moral rights for the publications made accessible in the public portal are retained by the authors and/or other copyright owners and it is a condition of accessing publications that users recognise and abide by the legal requirements associated with these rights.

- Users may download and print one copy of any publication from the public portal for the purpose of private study or research.
- You may not further distribute the material or use it for any profit-making activity or commercial gain
- You may freely distribute the URL identifying the publication in the public portal

If you believe that this document breaches copyright please contact us providing details, and we will remove access to the work immediately and investigate your claim.

Author's Accepted Manuscript

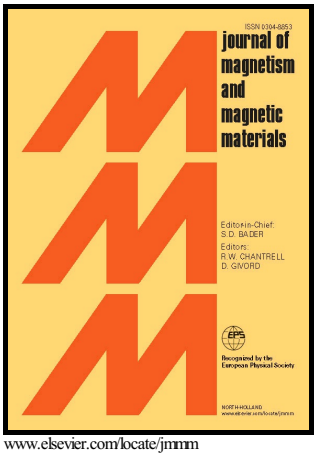

www.elsevier.com/locate/jmmm

The Effect of Nano-TiC Addition on Sintered Nd-Fe-B Permanent Magnets

Zorjana Mural, Lauri Kollo, Manlong Xia, Christian R.H. Bahl, Asger Bech Abrahamsen, Henrique Neves Bez, Joosep Link, Renno Veinthal

PII: S0304-8853(16)33495-3
DOI: http://dx.doi.org/10.1016/j.jmmm.2016.12.115
Reference: MAGMA62323

To appear in: *Journal of Magnetism and Magnetic Materials*

Received date: 18 April 2016
Revised date: 28 October 2016
Accepted date: 23 December 2016

Cite this article as: Zorjana Mural, Lauri Kollo, Manlong Xia, Christian R.H Bahl, Asger Bech Abrahamsen, Henrique Neves Bez, Joosep Link and Renno Veinthal, The Effect of Nano-TiC Addition on Sintered Nd-Fe-B Permanent Magnets, *Journal of Magnetism and Magnetic Materials* http://dx.doi.org/10.1016/j.jmmm.2016.12.115

This is a PDF file of an unedited manuscript that has been accepted for publication. As a service to our customers we are providing this early version of the manuscript. The manuscript will undergo copyediting, typesetting, and review of the resulting galley proof before it is published in its final citable form. Please note that during the production process errors may be discovered which could affect the content, and all legal disclaimers that apply to the journal pertain.

ACCEPTED MANUSCRIPT

The Effect of Nano-TiC Addition on Sintered Nd-Fe-B Permanent Magnets

Zorjana Mural[1*], Lauri Kollo[1], Manlong Xia[2], Christian R. H. Bahl[2], Asger Bech Abrahamsen[3], Henrique Neves Bez[2], Joosep Link[4] and Renno Veinthal[1]

[1]Department of Materials Engineering, Tallinn University of Technology, Ehitajate tee 5, 19086 Tallinn, Estonia
[2]Department of Energy Conversion and Storage, Technical University of Denmark, Frederiksborgvej 399, 4000 Roskilde, Denmark
[3]Department of Wind Energy, Technical University of Denmark, Frederiksborgvej 399, 4000 Roskilde, Denmark
[4]National Institute of Chemical Physics and Biophysics, Akadeemia tee 23, 12618 Tallinn, Estonia
[*]Corresponding author: zorjana.mural@ttu.ee

Abstract

This paper addresses the effect of nano-TiC addition on sintered Nd-Fe-B permanent magnets. TiC nanoparticles were added to sintered Nd-Fe-B magnets with a specific aim to improve the Curie temperature and thermal stability. A standard powder metallurgy route was adopted to prepare the magnets. It was found that introducing nano-TiC prior to jet milling was effective as the nanoparticles dispersed in the final alloy, concentcalcrating in the neodymium-rich phase of the magnets. Magnets with optimal properties were obtained with the addition of 1 wt% TiC nanoparticles. The hysteresis loop for such magnets showed an improved shape and VSM analysis a coercivity value of 1188 kA/m, a remanence value of 0.96 T and a maximum energy product of 132 kJ/m^3. The maximum working point and the Curie temperature of the developed magnets were 373 K and 623 K respectively.

Keywords: Sintered Nd-Fe-B magnets, magnetic properties, thermal stability, TiC

1. Introduction

Since the discovery of the $Nd_2Fe_{14}B$ compound in the 1980s [1], continuous efforts have been made to enhance not only the magnetic properties but also the thermal stability and corrosion resistance of Rare-Earth (RE)-based magnets. This aim can be reached by optimizing the microstructure and chemical composition of the magnets [2-5].

The largest application segments for Nd-Fe-B permanent magnets are expected to be those related to electric motors and power generation. These application areas require magnets that in addition to a reduced size and higher performance have an ability to work at high temperatures. Neodymium and iron are usually substituted by different elements to influence the properties of Nd-Fe-B magnets. In order to improve coercivity, anisotropy, corrosion behaviour or thermal stability of these magnets, various minor additives have been investigated. While a significant enhancement of coercivity occurs with the addition of Al, Cu, Nb, Tb, Ga, Dy_2O_3 or ZrO_2 to magnets, most of these elements lead to a decrease in remanence or thermal stability of the magnetic material [2-5]. Microalloying magnets with Co, V, Cr or Ni surpasses the corrosion issue of magnets but degrades their magnetic properties in some cases [6, 7].

Commonly, Dy is added to Nd-Fe-B magnetic material to ensure higher thermal stability. For Dy nanoparticle addition, the maximum effect of coercivity increase was reached at 1.5 wt%. A further addition of Dy appears not to remarkably increase the properties of Nd-Fe-B [8]. In case of micrometer-sized Dy powders**,** up to 10 wt% can be added to reach the same effect. Co is also known to positively influence the Curie temperature. Alloying with not more than 0.2 % of Co is recommended; otherwise, the saturation magnetization and anisotropy energy decreases. In order to supress the decrease in magnetic properties, it is recommended that apart from Co, other elements like copper or niobium should be added to the material. The replacement of Fe for Co improves the temperature coefficient, which will allow using such magnets in high temperature applications [9-13].

Most investigations in alloying have been focused only on the manufacturing stage of magnetic alloys, including strip casting and rapid quenching. Ti and C have been used separately or together to modify the Nd-Fe-B alloys. Minor additions of Ti and C resulted in an increase in coercivity with a modest decrease in remanence [14, 15]. The content of Ti and C should not exceed 3 at%; otherwise, the TiB_2 phase will appear instead of the TiC phase and decrease the volume of the

Accepted manuscript

ACCEPTED MANUSCRIPT

hard phase [14, 16]. TEM analysis showed Ti or Ti and C addition to produce finer and more homogeneous grains, which is beneficial for the coercivity of the magnet [17, 18]. Adding TiC to Nd-Fe-B alloys results in a more uniform microstructure with a strengthened exchange coupling effect [17, 19]. It was also found that due to a smaller grain size Nd-Fe-B-TiC bonded magnets absorb less hydrogen and have higher corrosion resistance characteristics [20].

This paper is aimed at analysing the effect of nano-TiC addition to sintered Nd-Fe-B magnets prior to the refining stage of a hydrogenated alloy with focus on the microstructure, thermal stability and magnetic properties of the doped Nd-Fe-B sintered magnets. To the authors' knowledge, this approach has not been reported in any previous research in the field.

2. Experimental

The conventional powder metallurgical route was adopted to produce sintered RE magnets. Commercial strip cast alloy in the form of flakes with the total RE content of 32 wt%, 67 % Fe and about 1 % B was applied as a starting material. The magnet alloy was Hydrogen Decrepitated (HD) at atmospheric pressure, and at room temperature with a holding time of 120 minutes. Jet milling (JM) under nitrogen atmosphere was performed, using the *Micromazinacione* spiral jet mill equipped with the *Impakt*^{TM} powder feeder by *Powder and Surface GmbH*. Nano-TiC powder with the average particle size of 20 nm (*SigmaAldrich*) weighing from 0.1 to 5.0 wt% was added to HD powder before feeding it into JM. The nanopowder was introduced by mixing the substance with a spoon. Cold isostatically pressed green compacts were sintered at 1353 K for 4 h under a vacuum of 10^{-5} mBar. The sintered magnets were slowly cooled down to room temperature with a total cooling time of approximately 3 h.

Magnetic properties at room and elevated temperatures were measured applying a Vibrating Sample Magnetometer (VSM) installed into the *Cryogenic Limited HTVSM 700* system with a maximum field of 14 T and a maximum temperature of 700 K. Demagnetization factors for rectangular samples to correct the measurements were calculated using analytic expression provided by Aharoni [21]. Sometimes descending and ascending hysteresis loops are not totally symmetrical due to instrument drift. In case of minor discrepancies in coercivity and remanence values, the hysteresis loop shifts were calculated and adjusted. Force calculations were based on the experimental information of magnetic moment, sample volume, demagnetization factor, and external and internal fields. Vacuum permeability was used to convert the measured data to the external field.

X-ray diffraction patterns were obtained using the *Rigaku SmartLab* diffractometer with Cu Kα radiation on crushed (powdered) samples placed on a silicon plate. The densities of the samples were measured by the *Micromeritics AccuPyc 1340* helium gas pycnometer, providing a skeleton density value. The phase concentration and the average grain size were analysed adopting the *ImageJ* software applied to Scanning Electron Microscope (SEM) micrographs. Energy Dispersive X-ray Spectroscopy (EDS) mapping was performed with the *Hitachi TM3000* electron microscope. Total oxygen content was determined by the *Eltra ONH2000* oxygen analyser for bulk samples of about 150 mg each as an average content of at least five measurements.

3. Results and discussion

3.1. Phase composition and density

X-ray studies were performed to identify the phase composition of the magnets and to clarify the influence of carbide on their microstructure. XRD measurements were performed for the sintered magnets with 0, 0.1, 0.5, 1 and 2 wt% of nano-TiC added as shown in Figure 1. The well-defined peaks were indexed as $Nd_2Fe_{14}B$ hard phase for all samples, refined with the Rietveld method. The black full lines indicate the measured data. It was not possible to identify the TiC phase for the samples with low dopant content up to 1 wt%. The analysis of XRD patterns showed single low intensity peaks corresponding to the TiC phase that were observed at approximately $2\theta = 36°$ and 61° for the samples with higher dopant content (1 and 2 wt%) [22]. It is important to note that phase quantification through XRD measurements is limited when the total content of the phase is less than 5 wt%.

Accepted manuscript

ACCEPTED MANUSCRIPT

The single peaks not defined by $Nd_2Fe_{14}B$ and TiC phases were observed at 2θ = 27°, 30° and 52°. The comparison of peak intensities at 2θ = 27° suggests that the secondary phase peaks are decreasing with increasing TiC concentration. This leads to a conclusion that the secondary phase corresponds to the Nd-rich phase or neodymium oxide since the amount of the Nd-rich phase decreases with increasing TiC content from about 11 % for the undoped sample to 7 % for the magnet with 1 wt% nano-TiC inclusion. Visually, it can be observed on microstructure figures in Figure 2 Section 3.2. Most probably the other single peaks correspond to the minor TiB_2 phase with the maximum peak at 2θ = 52°. As shown in Table 1, the total oxygen content appears to increase slightly for the samples with higher dopant concentration. This increase can be attributed to the oxygen pickup by finer intergranular RE regions and formation of oxides.

Lattice parameters of the hard magnetic phase were determined from the Rietveld refinement as demonstrated in Table 1. They are close to the values reported with a = b = 8.789 Å and c = 12.189 Å of the tetragonal $Nd_2Fe_{14}B$ unit cell [23]. There is practically no change in lattice parameters with the increase in additive concentration, which suggests that the hard magnetic phase is not doped with TiC and carbide particles behave as inclusions between the grains in RE-rich phase regions. It seems that TiC does not decompose during processing and acts as a grain refinement agent in the Nd-rich phase.

With increasing TiC content, the theoretically expected maximum density decreases by 2.4 % at the highest TiC content of 5 wt%. The relative skeleton density for the doped samples is in accordance with the expected maximum density shown in Table 1. Generally, with increasing TiC content, the density is slightly decreasing. All samples, except for the one with the highest TiC content of 5%, comply with the industrial standards in regard to the density of the magnet and can thus be used for further characterization.

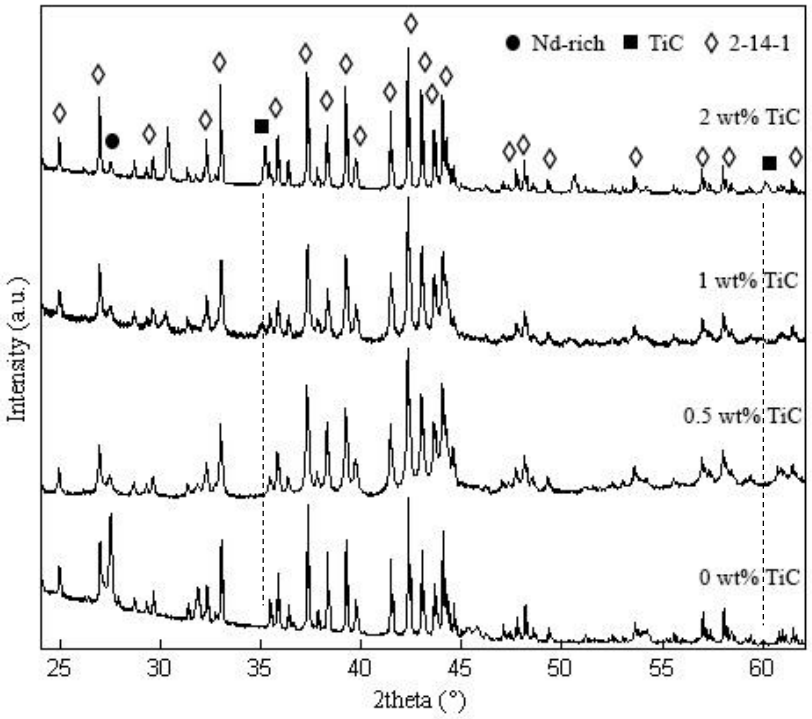

Figure 1. X-ray patterns of 0, 0.5, 1 and 2 wt% nano-TiC Nd-Fe-B sintered magnets.

Designation	a, b[Å]	c[Å]	Relative Density	Oxygen Content [wt%]
0TiC	8.792	12.176	0.99	0.22
0.1TiC	8.796	12.189	0.99	0.28
0.2TiC	-	-	0.94	0.29
0.5TiC	8.796	12.189	0.96	0.29
1TiC	8.797	12.179	0.96	0.30
2TiC	8.798	12.183	1.00	-

ACCEPTED MANUSCRIPT

5TiC	-	-	0.92	-

Table 1. Lattice parameters a, b and c of the Nd-Fe-B phase doped with TiC determined from Rietveld refinement of X-ray diffraction patterns. The relative density and oxygen content of the sintered magnets is also listed.

3.2. Microstructure

SEM-EDS was performed to determine the distribution of additives in the microstructure of the magnets. SEM images of the initial sample and 1 wt% nano-TiC containing sample are displayed in Figure 2a and 2b respectively, and EDS mapping of magnet with 1 wt% nano-TiC in Figure 2d. The lighter phases correspond to the mixture of RE-rich phases and the darker phase to the $Nd_2Fe_{14}B$. TiC-free samples have a coarser structure with an average grain size of about 8 μm (Figure 2a), whereas 1wt% nano-TiC addition produces a finer more homogeneous structure with an average grain size of about 6.5 μm and a lower percentage of nonmagnetic phase (Figure 2b). Figure 2c and EDS mapping of the Ti element (Figure 2d) indicate that this element is concentrated mostly in the RE-rich phase and in between of the grains and is almost not present in the hard phase. This result is in agreement with X-ray and Rietveld along with oxygen content (Figure 2d) results presented in the previous paragraph. The TiC particles look like thin long clusters (lamellas) lined along the grains (Figure 2c). The grain refinement can be explained by the effect of nano-TiC particles distributed between the grains acting as inhibitors of the grain growth. The proposed mechanism of microstructure development is illustrated in Figure 3. In Figure 2c two RE-rich phases can be clearly identified. The mapping of oxygen (Fig. 2d) indicate that less bright RE regions correspond to RE oxides, while bright areas surrounding the oxides (Fig. 2c) attributes to the metallic Nd as no oxygen has been detected. TiC particles occupy the regions rich of metallic Nd (Fig. 2c).

The elemental concentrations were determined by EDS quantitative analysis in the core of the $Nd_2Fe_{14}B$ grains and intergranular regions. It was found that the concentration of Ti varies significantly through the RE-rich region. Ti content was not higher than 0.4 wt% (±0.05 %) for the hard phase and varied between 1 (±0.1 %) and 13 wt% (±0.5 %) for the RE-rich phase. EDS quantification proved the carbide was not dissolved in the hard magnetic phase. Similar results that in comparison with the hard phase, where the Ti content was not more than 0.1 at.%, grain boundaries and triple junctions contained 2.8...45 at.% Ti have been reported in previous research [24]. EDS analysis revealed also a significant variability of oxygen content in different phases. Generally, for the hard phase the oxygen level was below the detection limit of EDS analysis. In RE-rich regions, the oxygen content reached 6…10 wt% with the measurement uncertainty of about 2 %. These measurements support the data addressed above in regard to the higher oxidation of the RE-rich phase and oxides mixture as minor phases.

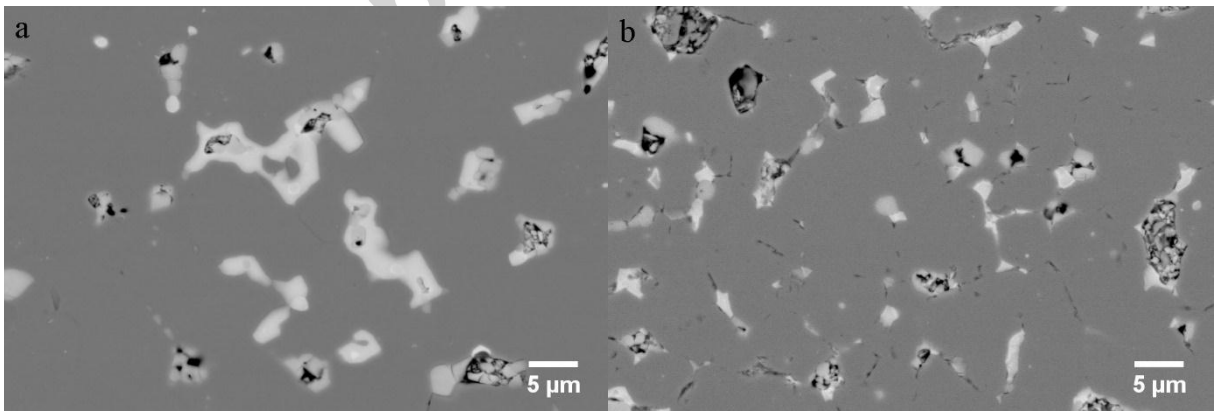

ACCEPTED MANUSCRIPT

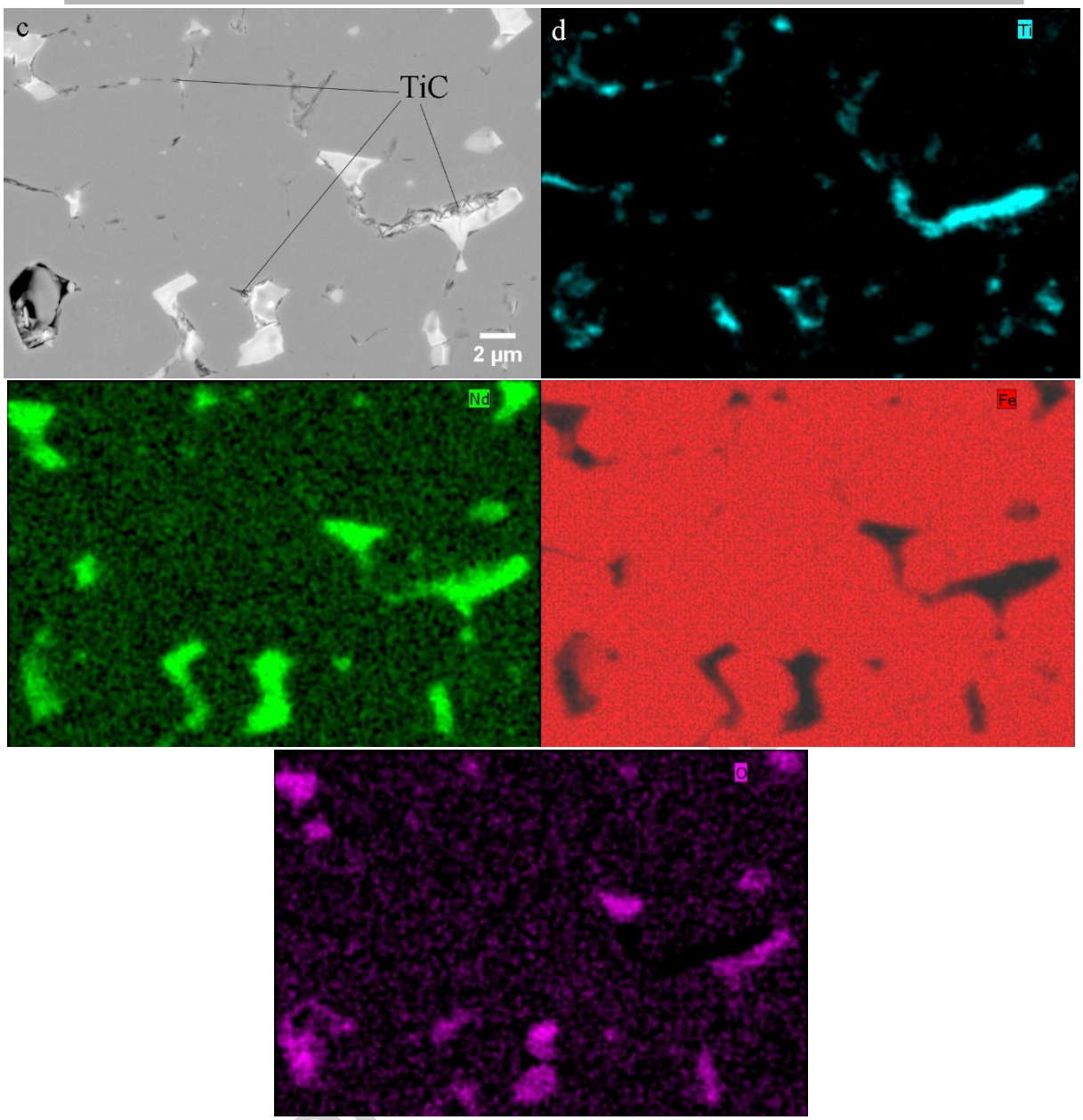

Figure 2. Microstructure: a) SEM image of the initial sintered magnet without TiC addition, b) sample with 1wt % of TiC, c) sample with 1 wt% of TiC, TiC particles are visible, d) EDS mapping of the whole area of the Figure 2c for Ti, Nd, Fe and O.

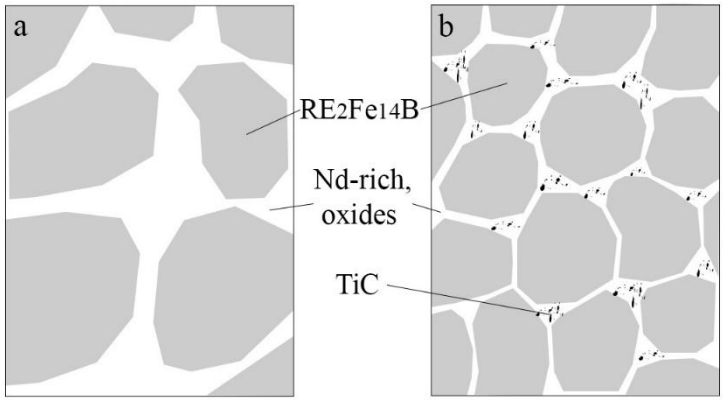

Figure 3. Mechanism of microstructure development with the magnet composition modified by TiC addition. Figure 3a provides a schematic illustration of the initial magnet. Figure 3b shows the influence of TiC addition.

ACCEPTED MANUSCRIPT

3.3. Magnetic properties

Magnetic properties of remanence (B_r), coercivity (H_{ci}) and maximum energy product (BH_{max}) measured at room temperature can be seen in Figure 4. In comparison to the samples without carbide, introducing a small amount of TiC causes a sudden decrease of remanence at TiC concentration 0.1 wt% and at the same time a remarkable increase in coercivity. The effect was confirmed with several experiments with the same additive concentration. This phenomenon is often caused by ineffective alignment of the powder during the production phase; however, this was not the case in this experiment. With the small concentration of 0.1 wt% TiC the difference in properties is quite significant, which may be related to the influential effect of nano particles. Generally, TiC has a positive influence on coercivity, which increases with TiC higher concentrations (Figure 4) and tends to decrease with TiC concentration exceeding 1 wt%. The remanence value remains nearly unchanged and it decreases with higher dopant concentrations at 2 and 5 wt% of carbide addition due to the nonmagnetic TiC phase. The maximum energy product is the highest for the magnet with 1 wt% TiC as can be seen in Figure 4.

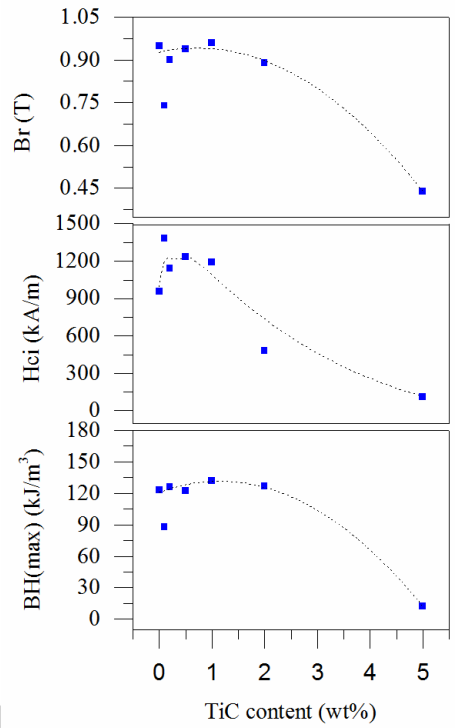

Figure 4. Magnetic properties of TiC doped Nd-Fe-B magnets at room temperature as a function of TiC content.

3.4. Thermal stability

Magnetic properties for sintered Nd-Fe-B magnets with TiC at elevated temperatures were measured. The second quadrant of the magnetization curves for the 1 wt% doped sample at temperatures from 293 to 498 K is shown in Figure 5. The temperature stability of magnetic materials is often described by the temperature coefficients for specific temperatures. The temperature coefficients for remanence α are defined by the difference in remanence divided by a temperature change multiplied by remanence at reference temperature:

$$\alpha = \frac{(B_r(T_r) - B_r(T))}{(B_r(T)) \cdot (Tr - T)}, \qquad (1)$$

where $B_r(T_r)$ refers to remanence at room temperature T_r and $B_r(T)$ to remanence at reference temperature T. The temperature coefficient of coercivity β is given by the difference in coercive strength divided by a temperature change times the coercivity at reference temperature:

ACCEPTED MANUSCRIPT

$$\beta = \frac{(H_{cj}(T_r) - H_{cj}(T))}{(H_{cj}(T)) \cdot (Tr - T)}, \qquad (2)$$

where $H_{cj}(T_r)$ refers to coercivity at room temperature T_r and $H_{cj}(T)$ to coercivity at reference temperature T [24]. The maximum operating temperature T_m was estimated as a temperature at which not more than 5 % loss of remanence occurred [26, 27]. The Curie temperature T_C was considered as a temperature at which remanence reached 0 T, because the Curie point is reached when the magnetic material changes its behaviour to paramagnetic [3, 25].

The temperature coefficients for remanence (α) and coercivity (β) together with the Curie temperature (T_C) and maximum operating (T_m) temperatures are displayed in Table 2. Compared to the initial characteristics, the highest working temperature and the Curie temperature of 373 K and 633 K respectively are found for the magnet with 0.5 wt% nano-TiC. The magnet with 1 wt% TiC showed 10 K lower Curie temperature. The mechanism influencing the thermal stability improvement of magnets with TiC additions are not clearly defined and understood. Several reasons have been proposed. Zhang *et.al.* propose the maximum operating point being influenced only by the increase of coercivity inhibiting the reversal processes [16]. In accordance to Chin *et.al.*, alloying with Ti results in reduction of reversible losses at temperatures up to 498 K due to the intrinsic improvement of anisotropy field [28]. This allows magnets to work at higher temperatures for longer period of time. Goto et.al. propose the coercivity and consequently thermal stability improvement due to strain induced in $Nd_2Fe_{14}B$ lattice for TiC alloyed materials [29]. In addition, the ferromagnetic behaviour of RE-rich phases especially grain boundaries have been reported [30, 31]. Moreover, adding small amounts of V, Mo or W to Nd-Fe-B magnets results in formation of intergranular boride phases like V_2FeB_2, Mo_2feB_2 or WFeB acting as domain walls pinning sites and are responsible for increased coercivity and thermal characteristics. It is believed that similar TiFeB phase may occur [32, 33]. In the present work as TiC is situated in RE-rich areas, it is assumed to have the influence in there or at the grain boundaries. Curie temperature of the magnets is increased already with 0.1 wt.% of nanoTiC inclusion, and remains constant even with TiC inclusions up to 2 wt.%. As such phenomenon was not seen with micrometer sized TiC alloying, we believe the mechanism of increased thermal stability is related to solubility of TiC in RE-rich phase and in the grain boundaries. The mechanism could lay in increased internal strains in microstructure or altered grain boundaries. Revealing the exact mechanisms need further investigations in the future. VSM measurements made at 700 K proved the samples with TiC behave as ferromagnetics and show a weak magnetic loop while undoped sample became nonmagnetic. Figure 6 shows the change of coercivity (b and d) and remanence (a and c) at high temperatures in terms of stability. The whole temperature range between 293 K and 673 K can be observed in graphs c and d and losses at lower temperatures (293…523 K) in graphs a and b. At low temperatures the difference in remanence is not significant, but at elevated temperatures the magnets with nano-carbide are more stable. In respect to coercivity, the outcome is quite similar at higher temperatures, whereas at lower temperatures the coercive force decreases slightly faster. At temperatures higher than 598 K, coercivity becomes irregular and it is difficult to predict the total loss of the coercive force of materials. This can be confirmed by the temperature coefficients shown in Table 2.

The current trend in Nd-Fe-B magnet fabrication is to increase the thermal stability of RE magnets by Dy addition. However, the availability of Dy is quite critical and at higher Dy concentrations remanence decreases significantly. Diffusion technique is adopted to enrich just the boundaries of $Nd_2Fe_{14}B$ grains with Dy; however, the size of these magnets is limited to several millimetres only [34]. TiC addition can become an alternative to Dy doping in order to improve the thermal properties of magnets. A benefit of introducing TiC nanoparticles into RE magnets composition lies in a possibility to mix the nanoparticles after casting the strip cast flakes of the magnetic alloy.

Accepted manuscript

ACCEPTED MANUSCRIPT

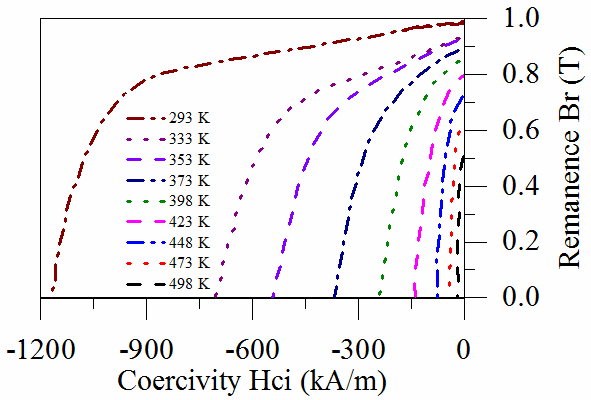

Figure 5. Second quadrant magnetization curves of 1 wt% TiC containing magnet at different temperatures.

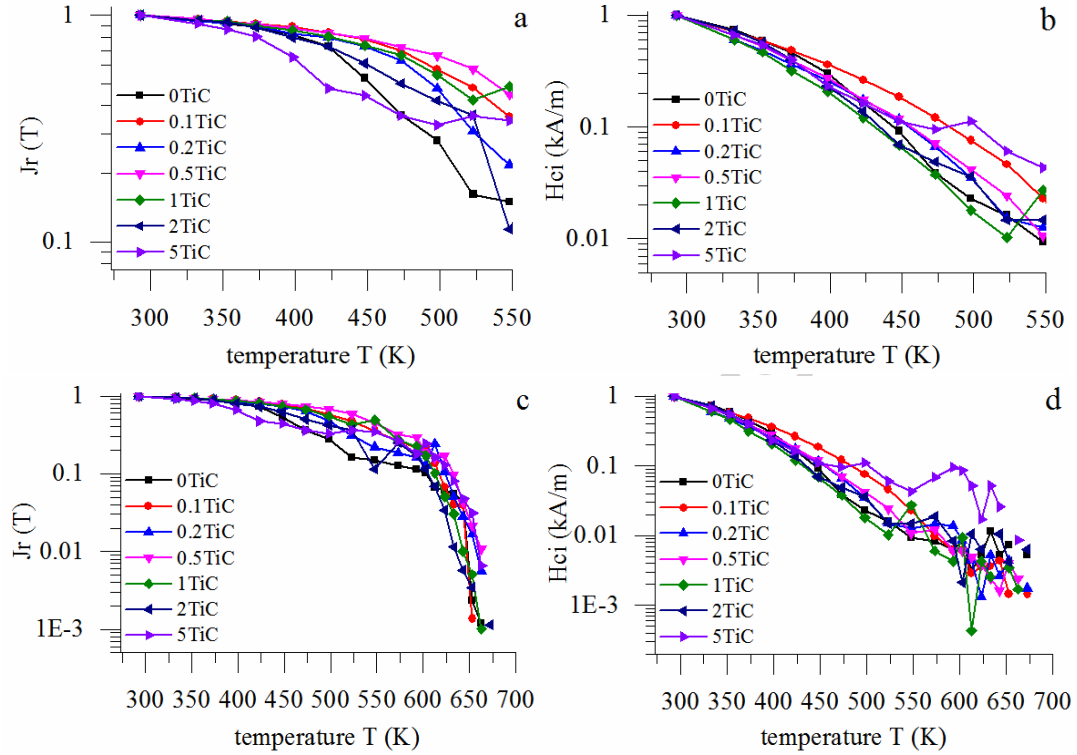

Figure 6. Temperature dependence of remanence (a and c) and coercivity (b and d) for magnets with different TiC addition levels. Figures 6a and 6b show lower temperatures region (293…523 K) while Figures 6c and 6d show the whole range of temperatures (293…673 K).

Designation	α[%/K]	β [%/K]	Tm [K]	Tc [K]
	373 K	373 K		
0TiC	-0.148	-1.466	333(±5)	583(±10)
0.1TiC	-0.112	-1.338	353(±5)	613(±10)
0.2TiC	-0.139	-2.184	373(±5)	623(±10)
0.5TiC	-0.116	-1.912	373(±5)	633(±10)
1TiC	-0.098	-2.699	373(±5)	623(±10)
2TiC	-0.160	-1.852	353(±5)	603(±10)
5TiC	-0.306	-1.902	333(±5)	593(±10)

Table 2. Temperature coefficients, the maximum working point and the Curie temperature

4. Conclusions

ACCEPTED MANUSCRIPT

This paper examined the effect of 0.1…5 wt% TiC nanoparticles addition into Nd-Fe-B sintered magnets on their magnetic properties, thermal behaviour and microstructure. According to the findings obtained in the research, the following conclusions can be drawn:

1. In the main, TiC particles are concentrated intergranularly in the RE-rich phase and show almost no evidence of dissolving in the main phase. Already at as small concentrations as 0.1 wt.% TiC nanopowder additions lead to a finer microstructure and decreased volume fraction of the nonmagnetic phase.
2. The addition of nano-TiC to RE magnets by mixing the carbide together with hydrogen decrepitated strip cast powder produced an improvement of their magnetic properties, in particular coercivity. The concentration of up to 1 wt% of nano-TiC appears to increase coercivity without a significant decrease in remanence.
3. The hysteresis loop for magnets doped with 1 wt% TiC generated properties as follows: coercivity 1188 kA/m, remanence 0.96 T and maximum energy product 132 kJ/m^3.
4. TiC addition can significantly improve the thermal stability and the Curie temperature of the magnet. At 1 wt% of nano-TiC the Curie temperature T_C can be raised to 623 K.

Acknowledgements

This research has been partially supported by a project "Permanent magnets for sustainable energy application (MagMat)" financed by the European Regional (Social) Fund under project 3.2.1101.12-0003 in Estonia. This work is part of the REEgain Innovation Consortium funded by the Innovation Fund Denmark (www.REEgain.dk).

A special gratitude should be given to Molycorp Silmet R&D Director Ms Jane Paju for providing experimental materials, assisting in characterization and supporting the research team throughout the project.

References

1. M. Sagawa, S. Fujimura, N. Togawa, H. Yamamoto, Y. Matsuura, New material for permanent magnets on a base of Nd and Fe, J. Appl. Phys. 55 (1984) 2083-2087.
2. S. Pandian, V. Chandrasekaran, G. Markandeyulu, K. J. L. Iyer, K. V. S. Rama Rao Effect of Al, Cu, Ga, and Nb additions on the magnetic properties and microstructural features of sintered NdFeB, J. Appl. Phys. 92 (2002) 6082-6086.
3. J. M. D. Coey, Rare-Earth Iron Permanent Magnets, Claredon Press Oxford, Oxford, 2006.
4. J. P. Nozieres, R. Perrier de la Bathie, Hot worked Nd-Fe-B permanent magnets: effect of additional element such as Dy, Si, Ce, Ti, Co and others, IEEE Trans. Magn. 25 (1989) 4117 – 4119.
5. L. Q. Yu, J. Zhang, S. Q. Hu, Z. D. Han, M. Yan, Production for high thermal stability NdFeB magnets, J.Magn. Magn. Mater. 320 (2008) 1427-1430.
6. P. Tenaud, F. Vial, M. Sagawa, Improved corrosion and temperature behaviour of modified Nd-Fe-B magnets, IEEE Trans. Magn. 26 (1990) 1930 - 1932.
7. H. Bala, G. Pawlowska, S. Szymura, V. V. Sergeev, Yu. M. Rabinovich, Corrosion characteristics of NdFeB sintered magnets containing various alloying elements, J. Magn. Magn. Mater. 87 (1990) 255-259.
8. W. Q. Liu, H. Sun, X. F. Yi, X. C. Liu, D. T. Zhang, M. Yue, J. X. Zhang, Coercivity enhancement in Nd-Fe-B sintered permanent magnet by Dy nanoparticles doping, J. Alloys Compd. 501 (2010) 76-69.
9. A. S. Kim, F. E. Camp, Effect of minor grain boundary additives on the magnetic properties of NdFeB magnets, IEEE Trans. Magn. 31 (1995) 3620-3622.
10. G. Bai, R. W. Gao, Y. Sun, G. B. Han, B. Wang, Study of high-coercivity sintered NdFeB magnets, J. Magn. Magn. Mater. 308 (2007) 20-23.
11. Y. Matsuura, S. Hirosawa, H. Yamamoto, S. Fujimura, M. Sagawa, Magnetic properties of the $Nd_2(Fe_{1-x}Co_x)_{14}B$ system, Appl. Phys. Lett. 46 (1985) 306-310.

Accepted manuscript

ACCEPTED MANUSCRIPT

12. F. E. Camp, A. S. Kim, Effect of microstructure on the corrosion behaviour on NdFeB and NdFeCoAlB magnets, J.Appl. Phys. 70 (1991) 6348-6350.
13. M. Sagawa, S. Fujimura, H. Yamamoto, Y. Matsuura, K. Higara, Permanent magnets materials based on the rare-earth-iron-boron tetragonal compounds, IEEE Trans. Magn. 20 (1984) 1584-1589.
14. D. J. Branagan, R. W. McCallum, Precipitation phenomenon in stoichiometric $Nd_2Fe_{14}B$ alloys modified with titanium and titanium with carbon, J. Alloys Compd. 230 (1995) 67-75.
15. C. H. Chiu, H. W. Chang, C. W. Chang, W. C. Chang, The effect of Ti and C on the phase evolution and magnetic properties of $Pr_9Fe_{bal}Ti_xB_{11-y}C_y$ (x = 0–4, y = 0–11) nanocomposites, J. Appl. Phys. 99 (2006).
16. R. Zhang, Y. Liu, J. Li, S. Gao, M. Tu, Effect of Ti&C substitution on the magnetic properties and microstructures of rapidly-quenched NdFeB alloy, Mater. Charact. 59 (2008) 642-646.
17. P. Haijun, Z. Maocai, B. Xiaoqian, Effect of doping of Ti and C on crystallization and magnetic properties of NdPrFeB thick melt-spun ribbons, Rare Metal Mat.Eng. 41 (2012) 212-214.
18. W. Cong, G. ZhiMeng, S. YanLi, B. XiaoQian, C. ZhiAn, Effect of titanium substitution on magnetic properties and microstructure of nanocrystalline monophase Nd-Fe-B Magnets, J. Nanomater. 2012 (2012).
19. M. J. Kramer, C. P. Li, K. W. Dennis, R. W. McCallum, C. H. Sellers, D. J. Branagan, L. H. Lewis, J. Y. Wang, Effect of TiC additions to the microstructure and magnetic properties of $Nd_{9.5}Fe_{84.5}B6Nd_{9.5}Fe8_{4.5}B_6$ melt-spun ribbons, J. Appl. Phys. 83 (1998) 6631-6633.
20. M. Arenas, G. W. Warren, C. P. Li, K. W. Dennis, R. W. McCallum, Corrosion and hydrogen absorption in melt Spun NdFeB-TiC bonded magnets, IEEE Trans.Magn. 33 (1997) 3901-3903.
21. A. Aharoni, Demagnetizing factors for rectangular ferromagnetic prisms, J. Appl. Phys. 83 (1998) 3432-3434.
22. R. O. Elliot, C. P. Kempter, Thermal expansion of some transition metals carbides, J. Phys. Chem. 62 (1958) 630-631.
23. L. X. Liao, Z. Altounian, D. H. Ryan, Cobalt site preferences in iron rare-earth-based compounds, Phys. Rev. B. 47 (1993) 230-241.
24. O. Filip, R. Hermann, L. Schultz, Growth kinetics and TiC precipitation phenomena in Nd-Fe-B-Ti-C melts in dependence on cooling parameters and composition, Mater. Sci. Eng. A. 375-377 (2004) 1044-1047.
25. R. Hilzinger, W. Rodewald, Magnetic Materials: Fundamentals, Products, Properties, Applications, Publicis Publishing, Erlangen, 2013.
26. S. R. Trout, Material selection of permanent magnets, considering thermal properties correctly, Proceedings of Electrical Insulation Conference and Electrical Manufacturing & Coil Winding Conference, (2001) 365-370.
27. Y. Kato, Thermal stability of sintered and bonded rare-earth magnets, J. Appl. Phys. 85 (1999) 4868-4870.
28. T. S. Chin, C. H. Lin, Y. H. Huang, J. M. Jau, Enhanced thermal stability of sintered (Nd, Dy)(Fe, Co)B magnets by the addition of Ta or Ti, IEEE Trans. Magn. 29 (6) (1993) 2788-2790.
29. R. Goto, K. Takagi, A. Hosokawa, K. Ozaki, Proceedings of the 24th International Workshop on Rare-Earth and Future Permanent Magnets and Their Applications (REPM 16), Darmstadt, Germany, (2016)
30. Y. Murakami, T. Taginaki, T. T. Sasaki, Y. Takeno, H. S. Park, T. Matsuda, T. Ohkubo, K. Hono, D. Shindo, Magnetism of ultrathin intergranular boundary regions in Nd–Fe–B permanent magnets, Acta Mater. 71 (2014) 370-379.
31. H. Sepehri-Amin, T. Ohkubo, T. Shima, K. Kono, Grain boundary and interface chemistry of an Nd–Fe–B-based sintered magnet, Acta Mater. 60 (2011) 819-830.
32. T. Y. Chu, T. S. Chin, C. H. Lin, J. M. Yao, Evidence of domain-wall pinning in W-doped (NdDy)(FeCo)B sintered magnets, J. Appl. Phys. 76 (1994) 6834-6836.
33. J. Bernardi, J. Fidler, F. Födermayr, The effect of V or W additives to microstructure and coercivity of Nd-Fe-B based magnets, IEEE Trans. Magn. 28 (5) (1992) 2127-2129

Accepted manuscript

ACCEPTED MANUSCRIPT

34. K. Löewe, C. Brombacher, M. Katter, O. Gutfleisch, Temperature-dependent Dy diffusion processes in Nd–Fe–B permanent magnets, Acta Mater. 83 (2015) 248-255.

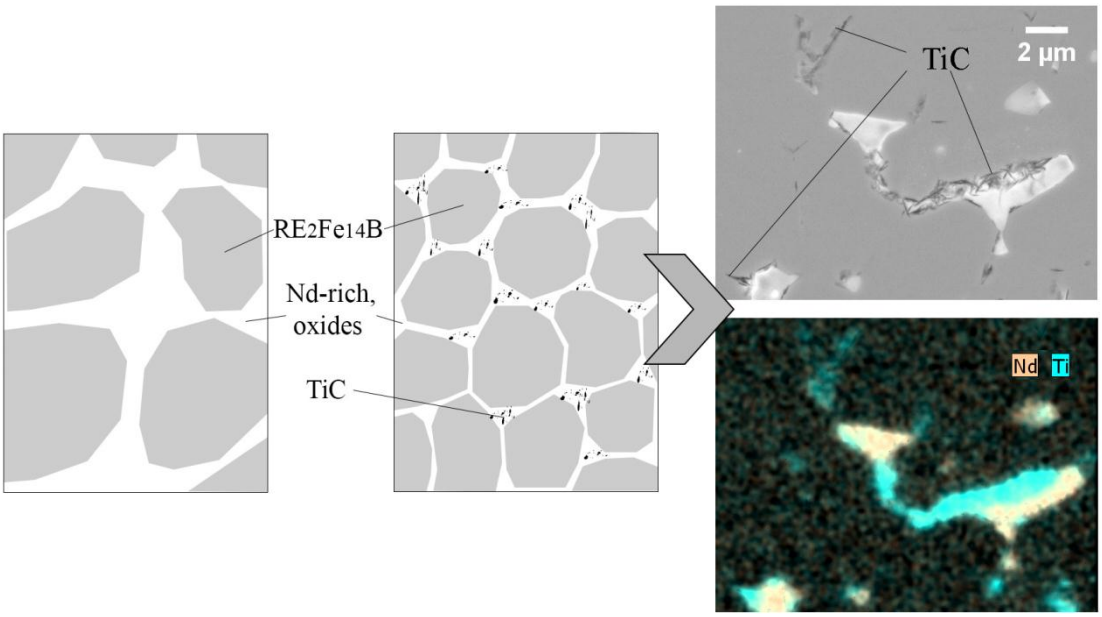

Highlights

- Improvement of thermal stability of Nd-Fe-B magnets by introducing nano-TiC prior sintering is proposed;
- The mechanism relies on nano-TiC particles behaving as grain growth inhibitors between thin RE-rich phase regions;
- The concentration of up to 1 wt% of nano-TiC appears to increase coercivity without a significant decrease in remanence;
- The maximum working point and the Curie temperature of the developed magnets are 373 K and 623 K respectively.

Accepted manuscript